Theor Chem Acc (2011) 128:807–823
DOI 10.1007/s00214-010-0857-9

REGULAR ARTICLE

Predicting binding energies of CDK6 inhibitors in the hit-to-lead process

Laura Delgado-Soler · Javier Ariñez-Soriano · José M. Granadino-Roldán · Jaime Rubio-Martinez

Received: 29 June 2010 / Accepted: 8 November 2010 / Published online: 8 December 2010

Abstract The main challenge for the "hit-to-lead" stage in the drug discovery process relies on the accuracy of existing docking methods. In fact, accuracy of docking methods depends not only on the scoring function used to rank the poses but also on the ability of the docking method to reproduce the experimental binding mode. At this purpose, the performance of different approximations to properly dock and score compounds with known activity in a narrow range of IC_{50} values was analyzed. A set of five ATP-competitive CDK6 inhibitors and three receptor conformations for CDK6 were considered for analysis, and three methodologies were used and analyzed in order to include different degrees of receptor flexibility. Thus, a completely rigid receptor is considered when using Glide, while the so-called Induced Fit Docking Protocol accounts for receptor sidechain rearrangements. Finally, force field calculations were also performed in order to consider a completely flexible receptor.

Published as part of the special issue celebrating theoretical and computational chemistry in Spain.

Electronic supplementary material The online version of this article (doi:10.1007/s00214-010-0857-9) contains supplementary material, which is available to authorized users.

L. Delgado-Soler · J. Ariñez-Soriano · J. Rubio-Martinez (✉)
Department de Química Física, Universitat de Barcelona (UB) and the Institut de Recerca en Química Teòrica i Computacional (IQTCUB), Martí i Franqués 1, 08028 Barcelona, Spain
e-mail: jaime.rubio@ub.edu

J. M. Granadino-Roldán
Departmento de Química Física y Analítica, Universidad de Jaén, Campus Las Lagunillas s/n, 23071 Jaén, Spain

Keywords Binding energy · Docking · CDK6 inhibitors · Drug design · MMPB/GBSA

1 Introduction

Recently, a vast amount of literature has been published, remarking the relevance of cell cycle deregulation in human cancer disorders [1]. Taken together, these abnormalities lead not only to an unscheduled cell proliferation but also to an increase in genetic alterations that may contribute to tumor progression or malignancy.

Cyclin-dependent kinases (referred to as CDKs) are responsible for the timing and coordination of the eukaryotic cell cycle. These proteins are inactive as monomers, and their activation requires binding to their regulatory subunits, known as cyclins. These latter constitute a diverse family of proteins that are synthesized and destroyed at specific times during the cell cycle, thus modulating CDK activity and cell cycle progression. CDK activity is increased in proliferative diseases such as cancer, frequently due to an overexpression of positive regulators (cyclins) or to the inactivation of CDK inhibitors. Thus, CDK inhibitors have been considered as relevant drug candidates for cancer therapy due to their potential for restoring the control of the cell cycle [2].

There is strong evidence that CDK2, CDK4, and CDK6 are not essential for the mammalian cell cycle since when any of these proteins is independently inhibited, the cell develops compensatory pathways to complete the division cycle [3]. However, they are required for the proliferation of specific types of cells, like tumor cells [1]. CDK4 and CDK6 are regulators of the G1/S transition during the cell cycle. Once the cell enters in the S stage, the division process is completed without any possible regulation by

extracellular signals. The importance of CDK2 as antitumoral target has been remarked in numerous publications. However, recent studies have shifted attention to CDK4 and CDK6 proteins because they act as earlier regulators of the cell cycle. Moreover, a better selectivity can be achieved when inhibiting these proteins in comparison with other CDKs such as CDK1 or CDK2 [4], which can be translated to a decrease in undesired side effects.

The search for small-molecule CDK inhibitors for cancer therapy has become an active field of research nowadays [5]. However, to date, no CDK inhibitors have been approved for commercial use [6]. The majority of reported CDK inhibitors are ATP-competitive. Unfortunately, undesired side effects associated with this kind of molecules are very frequent, which can be expected due to the huge number of protein kinases existing in a human organism. Different types of inhibitors have been described according to their activity profile against the CDK family, and there is a big controversy over the need to develop selective inhibitors. The principal drawback of selective inhibitors is their reduced potency since cell develops compensatory pathways. However, toxicity problems have also been described for pan inhibitors. Some references point to the combined therapy of CDK inhibitors with other cytotoxic agents as the best strategy for cancer treatment [6].

The main limitation for the design of selective inhibitors relies on the accuracy of docking methods for predicting the experimental binding affinities. The most accurate methods existing nowadays (i.e., thermodynamic integration or free-energy perturbation methods) have an approximate error of 1 kcal/mol [7]. This fact implies that a modern docking method with a typical 2–3 kcal/mol error, which corresponds to differences of three orders of magnitude in the IC_{50} values, should have some difficulties to properly rank a set of compounds with similar IC_{50} activities [8].

The accuracy of docking methods depends not only on the scoring function used to rank the poses but also on the ability of the docking method to reproduce the experimental binding mode. Docking programs usually incorporate empirical scoring functions that have been calibrated for a wide range of known active compounds and, despite the simplicity of these functions, they offer a reasonable performance considering the low computational cost required. However, accuracy of scoring functions only makes sense when analyzing the real binding mode. Receptor flexibility remains one of the major challenges for this field [9]. The most rigorous docking methods only include some local rearrangements or sidechain restructuration. Indeed, some authors suggest the need to use different receptor conformations for docking studies [9, 10] in order to properly account for receptor flexibility.

The goal of this work is to analyze the performance of different approximations to properly dock and score compounds with known activity within a narrow range of IC_{50} values. A set of five ATP-competitive CDK6 inhibitors and three receptor conformations for CDK6 were considered for analysis. Three methodologies were used in order to include different degrees of receptor flexibility. Thus, a completely rigid receptor is considered when using the Glide [11] module of the Maestro v9.0 suite of programs [12]. In addition, a new docking workflow named Induced Fit Docking Protocol [13] was used in order to account for receptor sidechain rearrangements. Finally, a completely flexible receptor was considered using force field calculations. These force field calculations required AMBER minimizations and molecular dynamics to obtain representative conformations of the different complexes obtained by receptor superposition. Later on, the MMPB/GBSA (molecular mechanics Poisson–Boltzmann/generalized Born surface area) methodology [14] was used to obtain the corresponding predicted binding energies.

2 Methods

2.1 Receptor modeling

The Protein Data Bank was used to search for structural information on CDK6 with ATP-competitive inhibitor complexes. As today, only three inhibitors have been co-crystallized with CDK6 and its activating protein (cyclin D). These are FSE (PDB ID 1XO2 [15]), AP9, and PD1 (PDB IDs 2F2C and 2EUF, respectively [16]). Other known CDK6 inhibitors, BYP and 2PU, have also been co-crystallized although in this case with the CDK2 protein (PDB IDs 1H08 and 1GIJ, respectively [17, 18]). The chemical names, structures, and IC_{50} values for these ligands when bonded to CDK6 can be found in Fig. 1 and Table 1, respectively.

Non-resolved residues in the FSE complex were modeled from other available structures of CDK6–cyclin D complexes; specifically, residues 124–126 of cyclin D were extracted from the structure with PDB ID 1BU2 [19] and residues 88–90 and 256–258 for CDK6 were found in structure with PDB ID 1G3N [20]. In order to relax the structure of these added residues and nearby zones and to eliminate close contacts, a minimization was performed in different steps. First, only added fragments were relaxed while constraining the remaining atoms. Next, receptor sidechains were minimized to accommodate new fragments. Finally, a whole-complex optimization was performed in order to allow possible backbone rearrangements. Once this complex was optimized, missing residues of the remaining two complexes (i.e., CDK6–cyclin D bound to

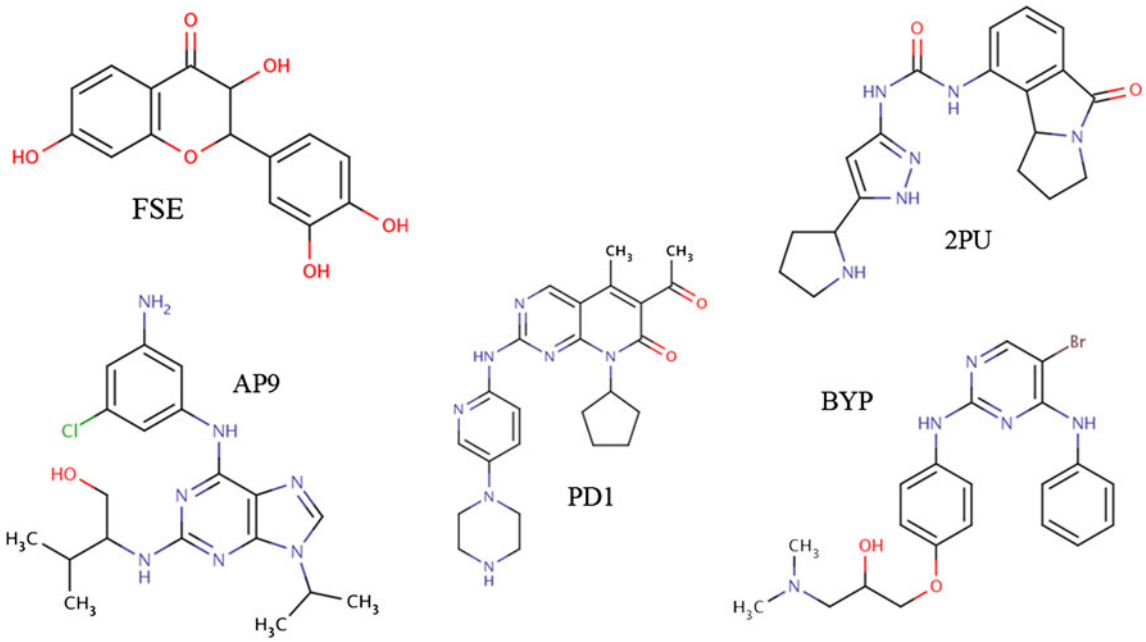

Fig. 1 Molecular structure of ligands studied

Table 1 Experimental IC_{50} values of studied ligands

Ligand	Chemical name	IC_{50} (nM)	Inhibited protein	Reference
FSE	Fisetin	850	CDK6	[15]
AP9	Aminopurvalanol	450	CDK6	[16]
BYP	(2R)-1-{4-[(4-anilino-5-bromopyrimidin-2-yl) amino]phenoxy}-3-(dimehylamino)propan-2-ol	~100	CDK4*	[17]
2PU	1-(5-oxo-2,3,5,9b-tetrahydro-1H-pyrrolo[2,1-a]isoindol-9-yl)-3-(5-pyrrolidin-2-yl-1H-pyrazol-3-yl)-urea	33	CDK6	[18]
PD1	PD0332991	10	CDK6	[16]

* Value for CDK4 inhibition. Due to the high sequence identity between these proteins, an equivalent value can be expected for CDK6

AP9 and PD1) were added from the FSE complex completed structure and equally minimized. These optimized complexes were used for further docking and force field calculation studies.

Minimizations were performed using the AMBER v.9 program package [21] with the parm99SB [22] parameter set for protein atoms and the GAFF force field [23] for ligands. AM1-BCC charges (Austin model 1-bond charge correction) were computed for the ligands using the ANTECHAMBER module within the AMBER package.

Initial complexes were soaked in a cubic box of explicit TIP3P water molecules [24] with a maximum distance between the protein and the edge of the box of 15 Å. Waters closer than 1.8 Å to any ligand or protein atom were removed. Finally, necessary counterions were added in order to neutralize the systems. Periodic boundary conditions were used in all simulations with the particle mesh Ewald method [25] to compute long-range electrostatic interactions. A cutoff distance of 10 Å was chosen to compute van der Waals (VDW) non-bonded interactions.

Once the complexes were modeled and minimized, receptors were aligned using the Superposition tool implemented in the Maestro v9.0 suite [12]. Residues further away than 5 Å from the ligand and with a defined secondary structure were used to superimpose minimized X-ray structures. After that, backbone RMSD was calculated for the above-mentioned motifs and, using also these superimposed coordinates, the RMSD was calculated for the part of each complex surrounding the binding site in order to quantify structural differences.

2.2 Ligand docking

Using the three CDK6–ligand complexes obtained from X-ray structure minimization together with the structural

information on BYP and 2PU bonded to CDK2, these five ligands were docked into the three modeled receptor conformations that arise after binding of CDK6 to different-sized ligands. Glide and Induced Fit Protocol, the latter adding some receptor flexibility, were the methods of choice to place each of the ligands on the CDK6 ATP-binding site. This allowed us to analyze the effects of binding site size and inclusion of flexibility.

2.2.1 Ligand and protein preparation

Before carrying out the docking step, ligand and protein structures must be prepared. Ligand bonds and formal charges were manually adjusted, and most representative ligand conformations and tautomers were generated by means of the LigPrep module of the Maestro v9.0 suite [26]. During this step, chirality and the original ionization state were preserved. Next, protein bonds and charges were assigned by the Protein Preparation tool with the exception of terminal residues, for which charges were manually added.

2.2.2 Glide

Glide module [11] allows performing all stages of a docking process, i.e., generation of ligand conformations, ligand docking, and scoring of the binding modes. As in this case a rigid receptor approximation is being used, it is expected that the different receptors considered will lead to different ligand-binding modes depending on the initial size of the ATP-binding cavity. Thus, the five known CDK6 inhibitors (FSE, AP9, BYP, 2PU, and PD1) were docked on the three available receptors following a multistep procedure (a more detailed protocol can be found in supporting information).

In order to describe receptor-binding properties, a grid of potential energy is calculated for atoms taking part of the binding pocket. These atoms are obtained from the analysis of each protein–ligand complex. In this step, default parameters were used. Then, the ligand is docked using the calculated grid to place it into the cavity and score the proposed binding modes.

2.2.3 Induced fit protocol

Using the previously prepared ligand and receptor structures, the Induced Fit Docking Protocol implemented in Maestro v9.0 [13] was also essayed in order to determine the effect of protein sidechain mobility inside the binding site. The choice of this protocol is based on its expected ability to model the conformational changes induced in the protein after ligand binding. This procedure follows a 4-step protocol: (1) We first use a softened van der Waals potential to dock the ligand into the rigid receptor and to generate an initial ensemble of poses. (2) After that, a protein sampling is conducted for each ligand pose using Prime. (3) Re-docking of the ligands into the best-ranked induced fit structures. (4) Finally, a scoring of the new ligand poses is performed using a combination of the Prime energy and Glide XP score.

The grid box computed in the Glide docking stage was centered on the bound ligands. Inner and outer box sizes were set to default values. No residue was found blocking the binding site, and thus, no alanine mutations were performed. Instead, in order to reduce steric clashes in a rigid receptor docking, all van der Waals radii for atoms in the binding site were scaled by 0.5. The 20 best-scored poses of the initial docking were refined using Prime. Only residues within 5 Å of the ligand were allowed to relax. Finally, each minimized structure was re-docked using Glide. All docking parameters were set to default values although XP precision in the scoring function was used. Only protein structures having energies in the range of 0–20 kcal/mol with respect to the lowest energy value produced by Prime were retained. An extended description of the whole docking protocol is available in supporting information.

2.2.4 Selection of the best-scored pose

Usually, binding affinities are thought to be related to the interaction energy between protein and ligand. In the case of the Glide docking procedure, this value is estimated by the empirical ChemScore-like function XP G-Score [27]. However, structures are ranked by default according to a model energy score function (E-Model in Glide or IFD Score in Induced Fit Docking) implemented in the docking protocol used. This value is supposed to be not only a measure of the interaction energy but also a measure of the stability of the generated complex. In the case of the E-Model function, the XP G-Score value is combined with the grid interaction score and the internal strain energy. For the Induced Fit Docking Protocol, an extra function has been included, i.e., IDF Score. This function combines the binding affinity predicted by XP G-Score with a 5% of the Prime energy found in the protein refinement calculation [28].

The choice of the best-docked structure for each ligand has been made according to different criteria, and rankings obtained were compared for the whole set of complexes. Then, two rankings were derived from Glide results: the first directly uses the E-Model function, which is intended to be more suitable for comparing the binding affinities of different ligands [29], and the second one uses the interaction energy as estimated by the XP G-Score function. In the case of the flexible docking process, rankings

equivalent to those obtained for Glide docking were attained and an extra ranking was obtained from the new IFD Score function, which is the chosen to rank poses by default.

In addition, RMSD was calculated among all structures resulting from each docking. Some studies suggest that usually the experimental binding mode corresponds to the most populated docking pose [30]. Thus, docking structures were clusterized using Ward's method [31] according to the RMSD value between them. For the selection of the best-scored pose, not only the scoring function was used: docking poses which appeared as isolated structures and cannot be included in any cluster were rejected as improbable conformations.

2.3 Force field calculations

2.3.1 Complex generation

All different starting points for molecular dynamics were directly obtained by superposition of all the experimental X-ray structures by means of the Protein Alignment Tool implemented in Maestro v9.0 [12]. Once all five crystallized structures were superimposed, ligand coordinates were transferred to each CDK6 receptor. Hence, a set of 15 complexes was obtained from five ligands positioned into three different conformations of the CDK6 binding site.

Complexes were solvated and neutralized as previously described. Force field parameterization and charges used were equivalent to those used in minimizations described above.

2.3.2 Energy minimization and molecular dynamics

The above-mentioned complexes were relaxed following a six-step minimization protocol in order to allow each ligand to accommodate in such different-sized binding cavities. During the three first steps, 5,000 steps of minimization using the steepest descent algorithm were done while restraining the protein backbone with harmonic force constants of 50, 5, and 0.5 kcal/mol^2 Å^2, respectively. Finally, other three stages consisting of 5,000 steps of minimization using the steepest descent algorithm followed by 5,000 steps using the conjugate gradient algorithm were performed without any restriction in order to complete the backbone relaxation. Parameters used were equivalent to those employed for the initial X-ray complex minimization.

In order to compare differences between ΔG values obtained from single-point calculations on the minimized complexes and those from a sampling of different conformations, molecular dynamics simulations were run for the three X-ray complexes previously minimized. These minimized structures were heated to 300 K at a constant rate of 30 K/10 ps while applying a harmonic restrain of 0.1 kcal/mol on protein backbone atoms. Once the systems were heated, each of them underwent two steps of 100 ps at constant pressure and without any restraints in order to increase its density. Finally, 5 ns of molecular dynamics were calculated within the NVT ensemble at a constant temperature of 300 K for each of the studied systems. Simulations were performed at constant temperature by coupling the systems to a thermal bath using Berendsen's algorithm [32] with a time coupling constant of 0.2 ps. Molecular dynamics simulations were run using the SHAKE algorithm [33] to constrain bonds involving the hydrogen atoms, hence allowing an integration time of 2 fs.

2.3.3 MMPB/GBSA approach

The molecular mechanics Poisson–Boltzmann/generalized Born surface area approach [14] (referred to as MMPB/GBSA) as implemented in the AMBER v.9.0 program package was used to estimate the binding affinities. Minimized complexes and structures extracted every 10 ps of molecular dynamics were used as representative conformations for free-energy analysis. The binding free energy is evaluated as

$$\Delta G_{\text{binding}} = \Delta G_{\text{gas}} + \Delta G_{\text{solv}} - T\Delta S$$

where ΔG_{gas} is the molecular mechanics interaction energy between protein and ligand. This interaction energy can be decomposed as a sum of non-bonded electrostatic (Coulombic), van der Waals (Lennard-Jones), and internal energy contributions (bonds, angles, and dihedrals) in vacuo. On the other hand, ΔG_{solv} is the solvation free energy and $-T\Delta S$ is the conformational entropy change.

ΔG_{solv} can be expressed as the sum of an electrostatic ($\Delta G_{\text{solv,elec}}$) and non-polar ($\Delta G_{\text{np}}$) components:

$$\Delta G_{\text{solv}} = \Delta G_{\text{solv,elec}} + \Delta G_{\text{np}}$$

The electrostatic contribution to the solvation free energy is directly computed solving the Poisson–Boltzmann (PB) equation in the case of MMPBSA, whereas the generalized Born (GB) approach [34] is used in MMGBSA. The non-polar contribution is assumed to be proportional to the solvent-accessible surface area (SASA). Hence, employing the LCPO method [35], the non-polar contribution is calculated as $\Delta G_{\text{np}} = \gamma$ SASA $+ \beta$, with $\gamma = 0.00542$ kcal/mol Å^2 and $\beta = 0.92$ kcal/mol for PB, and $\gamma = 0.0072$ kcal/mol Å^2 and $\beta = 0$ kcal/mol for GB calculations. Values of the internal and external dielectric constants were set to 1 and 80, respectively. Entropic contributions were also calculated using a normal mode analysis as implemented in the AMBER package. Before

the normal mode analysis, a Newton–Raphson optimization was performed on minimized complexes to achieve an RMSD lower than 10^{-4}. According to the GB parameterization used, atomic MMPBSA radii were set to mbondi2 [36].

3 Results and discussion

3.1 Receptor description

In order to determine pocket rearrangements in the three crystallized structures after ligand binding, relevant motifs of the CDK6 protein distant to the binding site were superimposed. Calculated RMSD values between superimposed residues are below 1 Å (specifically, 0.64 Å between the FSE and AP9 receptors, 0.95 Å between the FSE and PD1 receptor, and 0.63 Å between the AP9 and PD1 receptors), allowing to conclude that those parts of the protein do not show any significant differences within the studied receptor set. This confirms their utility as reference points for receptor superposition. However, RMSD values for residues of the binding pocket exhibit higher values (specifically, 1.44 Å for the AP9 and PD1 receptors, 2.10 Å for the FSE and AP9 receptors, and 2.29 Å for the FSE and PD1 receptors). When comparing RMSD values of residues belonging to the binding site region, it can be observed that AP9 and PD1 receptors share a relatively similar binding site structure. On the other hand, the conformation of CDK6 bound to FSE, adapted to the ligand's low size, significantly differs from the other two structures. Thus, as can be inferred from the inhibitor molecular volume, different-sized receptor cavities can be observed for the three X-ray experimental structures (see Fig. 2) and the inclusion of binding site flexibility in the docking methodology is expected to be determinant to reproduce the observed ability of the receptor to accommodate different types of ligands.

3.2 Ligand docking

3.2.1 Self-docking of the crystallized ligands

Focusing on the re-docking of each ligand into its bonded CDK6 receptor, it can be seen that energy functions (either E-Model or IFD Score, bold values in Tables 2, 4) lead to a proper ranking for the three crystallized ligands. However, when using the interaction energy (XP G-Score) to rank the poses, neither Glide nor the Induced Fit Docking Protocols reproduce the experimental binding affinities reported for these compounds. It is worth to note that Glide results are not improved when introducing receptor flexibility with the Induced Fit Docking Protocol. As each receptor is adapted to the docked ligand, sidechain receptor rearrangements are not relevant to achieve optimal interactions with the ligand with the energy function used.

In addition, rankings for all the compounds into the three receptor conformations were analyzed. Each scoring function used leads to a different compound ranking, the major part of them in disagreement with experimental data (see Tables 2, 3 for Glide docking and Tables 2, 3, 4 for Induced Fit Docking). Only the model structure derived from the X-ray structure of CDK6 with the PD1 inhibitor seems to provide some theoretical rankings which fully agree with activity data. CDK6 conformation when bound to the FSE receptor exhibits a narrow binding cavity which hinders the binding of bigger ligands (PD1 and AP9), even allowing sidechains to move during an Induced Fit Docking. Oppositely, AP9 cavity is too large, and despite ligands are easily embedded in, interactions are not as optimal as they would be with a backbone rearrangement. In conclusion, rearrangements allowed by the Induced Fit Docking are not enough to accommodate ligands in different-sized cavities, and only a medium-sized pocket would lead to reasonable results.

Among all the scoring functions considered, E-Model is the one that better fits the experimental ordering, either with the Glide rigid docking or with the Induced Fit Docking Protocol (Table 2). Considering the interaction energy criterion, the value of the best-scored pose according to the XP G-Score function (Table 3) does not reproduce any of the experimental binding affinities. The new energy function introduced in the Induced Fit Docking Protocol, IFD Score, only seems to provide reasonable results for the PD1 receptor. As Prime refinement energy is almost a constant value for all the structures, the IFD criterion (Table 4) is completely equivalent to the XP G-Score function, which neither reproduces the experimental activity ranking.

Focusing on the E-Model scoring function, reasonable results can be obtained when taking into account the binding size cavity and method flexibility. The structure of the CDK6 binding pocket bound to the FSE ligand hinders the docking of bigger ligands. Scoring values obtained are in disagreement with experimental data, especially when using rigid docking, as the binding site cavity is not big enough to accommodate these ligands. This does not happen in the case of CDK6 bound to PD1 and AP9 structures, which are already adapted to bigger ligands. However, the CDK6 bound to AP9 structure does not provide a proper ranking when using Glide docking due to the fact that the rigid receptor hypothesis does not allow pocket rearrangements to accommodate ligands and hence the docking fails for small ligands. With the Induced Fit Docking Protocol, reasonable results are obtained as inclusion of sidechain flexibility allows to better

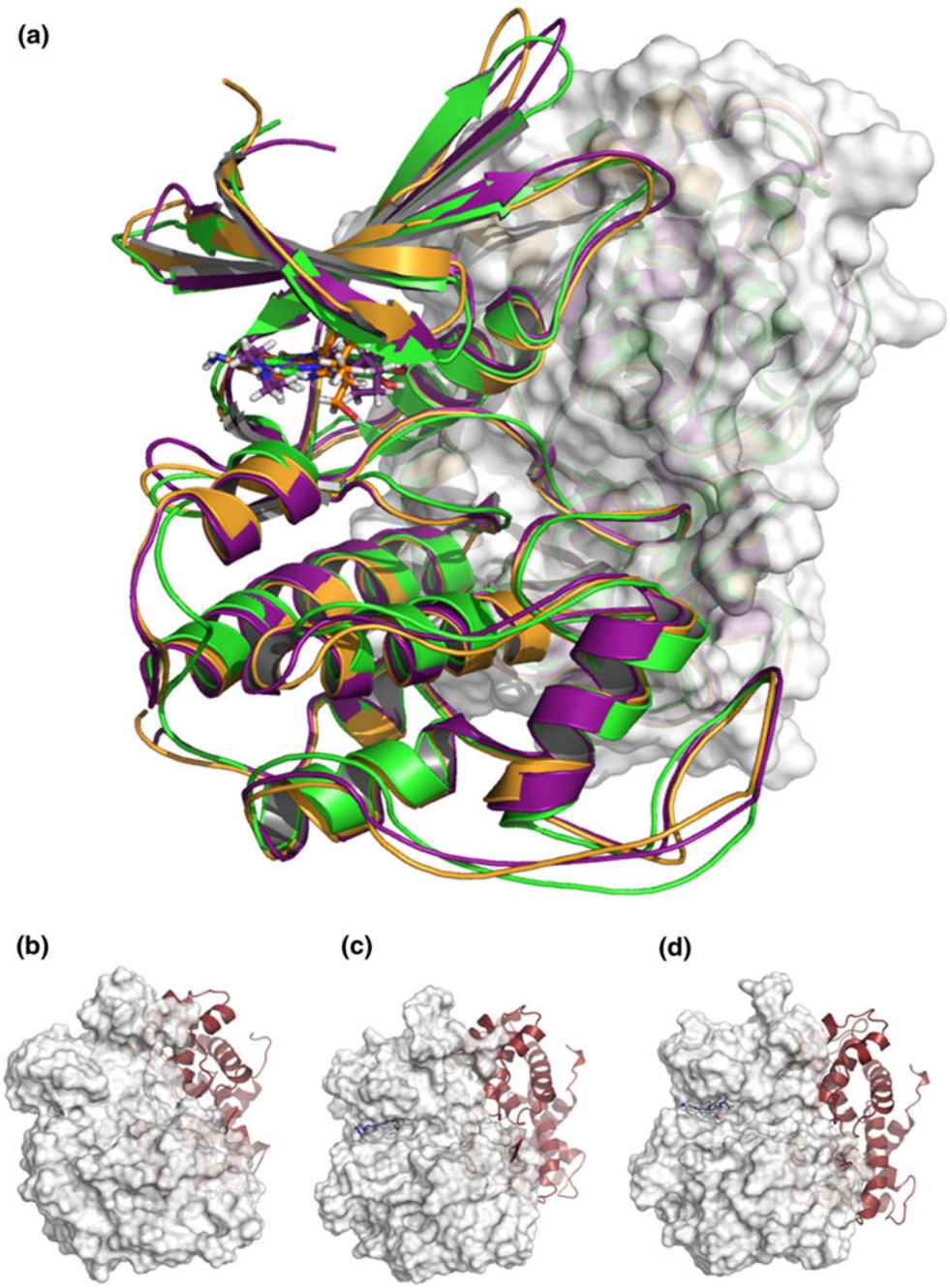

Fig. 2 **a** X-ray structures of the CDK6 protein in complex with three ATP-competitive inhibitors. FSE complex structure is depicted in *green*, AP9 in *orange*, and PD1 in *purple*. Differences in binding site size are significant among the complexes and are shown using molecular surface representation for the CDK6 protein in **b** FSE complex, **c** PD1 complex, and **d** AP9 structure

accommodate ligands into the binding pocket. The best results are obtained with the structure from CDK6 bound to PD1, the medium-sized ligand, which, due to the ligand size, exhibits an optimal pocket to dock the panel of ligands studied. E-Model ranking completely agrees with IC_{50} data either in the rigid Glide docking or in the Induced Fit Docking Protocol.

Thus, it can be concluded that completely different rankings were obtained with different essayed score functions, the majority in disagreement with experimental IC_{50} values. The interaction energy provided by the XP G-Score function is not the only factor to be considered in order to reproduce the experimental activity. The score obtained during the grid stage seems also to be a relevant contribution to obtain a proper ranking as shown for E-Model values. However, effects of receptor rearrangements estimated by Prime energy and included in the IFD score are not significant enough to properly modify the XP G-Score values and provide a proper ligand ranking.

In addition, a dependency between ligand ranking and the receptor structure used is found, which can be related to the size of the binding site cavity. Even in the case of the

Table 2 E-Model values for the best-scored pose in Glide docking (Glide) and the Induced Fit Docking Protocol (IFD)

Ligand	CDK6_FSE		CDK6_AP9		CDK6_PD1	
	Glide	IFD	Glide	IFD	Glide	IFD
FSE	**−88.1**	**−95.89**	−65.2	−75.95	−60.0	−68.38
AP9	−60.0	−92.65	**−90.4**	**−101.57**	−78.3	−91.75
BYP	−78.3	−105.35	−84.9	−89.85	−80.5	−96.12
2PU	−60.9	−115.87	−81.8	−107.92	−85.4	−106.00
PD1	−30.1	−108.69	−101.1	−112.54	**−98.3**	**−109.08**

Bold values correspond to the X-ray complexes

Table 3 Best XP G-Score value for poses obtained from the Glide docking (Glide) and the Induced Fit Docking Protocol (IFD)

Ligand	CDK6_FSE		CDK6_AP9		CDK6_PD1	
	Glide	IFD	Glide	IFD	Glide	IFD
FSE	**−14.39**	**−13.72**	−12.70	−10.77	−11.40	−10.06
AP9	−7.71	−11.17	**−13.67**	**−12.78**	−9.60	−10.90
BYP	−13.87	−12.31	−14.23	−11.27	−10.96	−10.23
2PU	−13.03	−11.30	−12.61	−11.57	−11.94	−12.34
PD1	−6.97	−11.02	−13.91	−13.08	**−14.46**	**−11.95**

Bold values correspond to the X-ray complexes

Table 4 IDF-Score values for the best-scored pose in Induced Fit Docking Protocol

Ligand	CDK6_FSE	CDK6_AP9	CDK6_PD1
FSE	**−974.8**	−972.5	−978.3
AP9	−972.3	**−976.9**	−980.1
BYP	−977.5	−977.4	−981.5
2PU	−971.3	−972.1	−978.4
PD1	−970.5	−975.2	**−979.1**

Induced Fit Docking Protocol, receptor flexibility is constrained and it can be thought that the binding cavity size biases the ligand binding. Thus, these results point to the fact that trying to perform a docking calculation using quite different sizes between receptor and ligand may lead to improper docking results.

In order to be compared to the experimental X-ray structure, RMSD was calculated between the best-scored Induced Fit Docking pose of FSE, AP9, and PD1 and the crystal structure (values shown in Table 5). It is worth to note that the three ligands docked in its own receptor reproduce the X-ray binding mode, with a maximum RMSD between theoretical and experimental structures of just 2.34 Å. Following the two aforementioned criteria, the most probable docking had a RMSD value of 0.42, 0.92, and 2.34 Å for the FSE, PD1, and AP9 complexes,

Table 5 RMSD values (Å) between the selected docking pose and the experimental X-ray structure

Ligand	CDK6_FSE	CDK6_AP9	CDK6_PD1
FSE	0.42	28.00	30.79
PD1	30.44	4.04*	0.92
AP9	27.68	2.34	3.41

* The fist best-scored pose according to E-Model criteria was an isolated structure and thus was discarded. The RMSD for this pose with respect to the X-ray structure was 9.32 Å

respectively. The higher value obtained for AP9 structure can be attributed to the fact that the CDK6 receptor has an opened conformation, which allows multiple ligand-binding modes. This fact, combined with the ligand flexibility, results in a huge number of possibilities for ligand positioning that hinders the reproduction of the real binding mode.

3.2.2 *Cross-docking calculations*

Cross-docking results of the three ligands into the three receptor conformations were also analyzed. When considering RMSD values for poses of dockings into receptor conformations not adapted to the docked ligands, bigger differences were found with the X-ray conformation (RMSD values near 30 Å in the worst cases). In the best cases (AP9 docked into the PD1-bonded receptor and viceversa), a relatively similar conformation was obtained (with an RMSD of 3.41 and 4.04 Å, respectively). Considering that both ligands have a similar size, it seems probable that docking in any of their bonded receptors will lead to reasonable results for both ligands. Focusing on the FSE ligand, neither its docking into the other receptor conformations nor the docking of other ligands into the FSE-bonded receptor are suitable situations for the docking protocol. Size differences between ligand and the binding cavity make ligand binding difficult. On the one hand, for small ligands, the number of possibilities to bind into a big cavity is enormous and the score function is not accurate enough to determine the best one. On the other hand, big ligands that must be embedded into small cavities, as the FSE binding pocket, usually find restrictions to achieve the real bonded conformation.

Best-scored poses for crystallized ligands docked into the three receptor conformations were visually compared to the experimental X-ray structure (structures depicted in Fig. 3). The receptor ability to accommodate ligands in different-sized cavities was only analyzed for the flexible docking results (Induced Fit Docking), having in mind that even in this case, receptor backbone mobility is restrained and only sidechains of residues within 5 Å of the ligand are allowed to move.

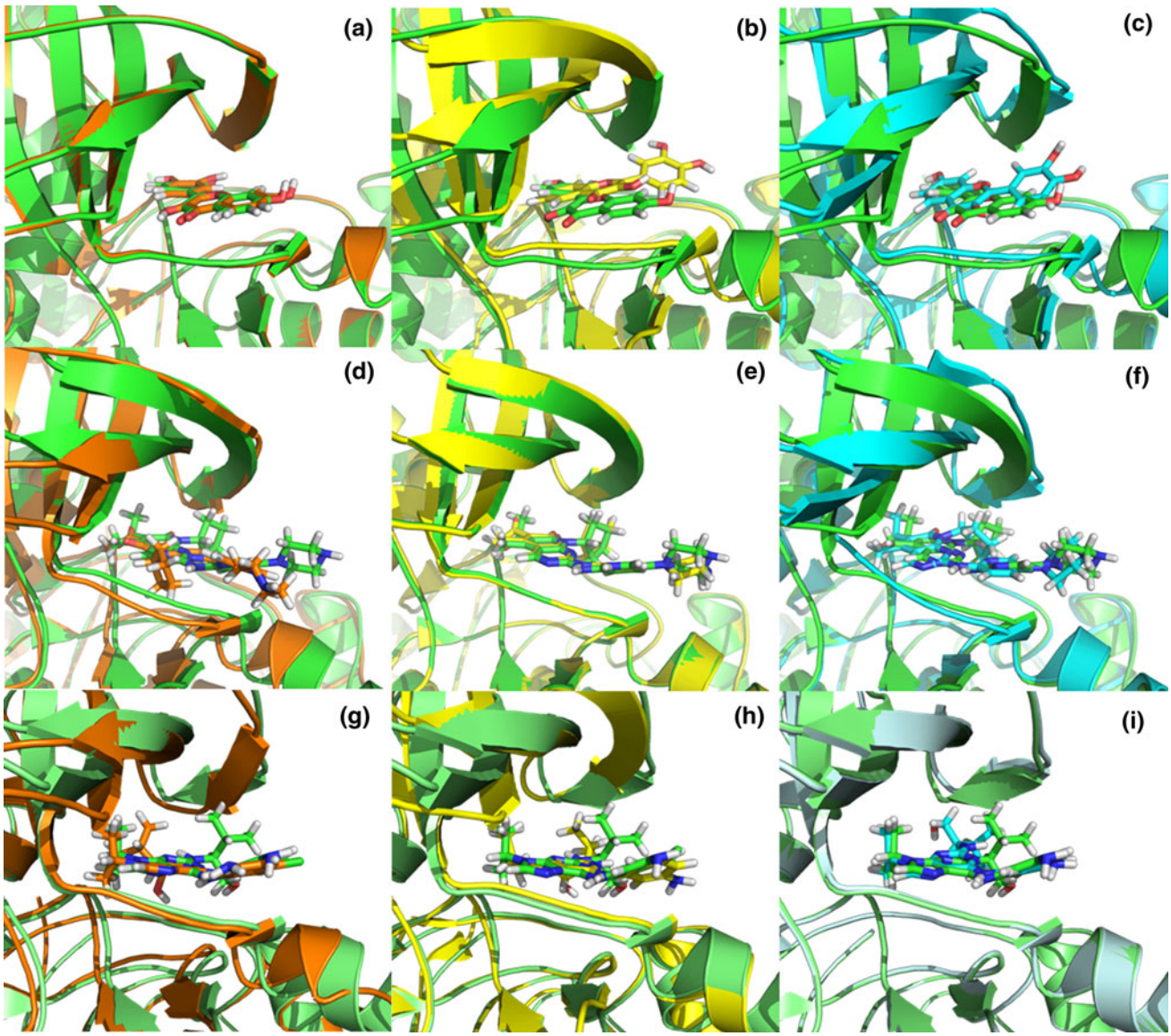

Fig. 3 Comparison between experimental X-ray structure and the best-scored docking poses for: **a** FSE into receptor bonded to FSE, **b** FSE into receptor bonded to PD1, **c** FSE into receptor bonded to AP9, **d** PD1 into receptor bonded to FSE, **e** PD1 into receptor bonded to PD1, **f** PD1 into receptor bonded to AP9, **g** AP9 into receptor bonded to FSE, **h** AP9 into receptor bonded to PD1, and **i** AP9 into receptor bonded to AP9

Indeed, when analyzing the worst docking results corresponding to FSE poses, it was found that these conformations were not as different from the X-ray structures as could be expected from the RMSD value (the calculated RMSD was near 30 Å). In the case of the AP9-bonded receptor docking, the FSE pose is rotated 180° with respect to the experimental conformation, which is reasonable due to the high ligand symmetry. Also, interactions observed for both poses are completely equivalent. Only small differences can be observed in the phenyl ring, as in order to achieve an extra H-bond, the ring appears slightly rotated. In the case of the PD1-bonded receptor, the ligand conformation is similar to the AP9 receptor, but the ligand is displaced in order to maintain the same extra H-bond discussed for the AP9 receptor docking pose. In the case of the PD1 receptor conformation, the region that establishes this extra bond seems to be further away and the ligand conformation is adapted to these differences. Similar differences are found for dockings of PD1 and AP9 into the FSE-bonded receptor. Symmetric regions of the ligands are rotated leading to a huge RMSD value. However, docked and experimental conformations are not so different. When comparing dockings of AP9 into PD1 bonded receptor conformation or vice versa, only small changes in the

position of some ligand groups are found. As receptor cavities and ligands have a similar size, docking structures are very similar to the experimental ligand conformation.

Thus, it can be said that the described docking protocol seems to lead to realistic structures. However, some considerations must be taken into account when there is no experimental structure to validate results. Docking protocols analyzed do not include a whole flexible receptor. Thus, in order to obtain reliable results, the receptor must be selected according to its binding cavity size, which should be similar to the ligand size. It has also been confirmed that isolated poses are not representative for the bonded ligand and that only populated poses must be taken in consideration as potential binding modes.

3.3 MMPB/GBSA calculations

In order to test the MMPB/GBSA methodologies, the three experimental available structures were initially minimized. To adapt the structures to the force field parameters, a complete structural relaxation was performed. However, neither MMPBSA nor MMGBSA binding energies calculated for the minimized structures were able to properly rank ligands according to their experimental activity (bold values in Tables 6, 7). The inclusion of entropic contributions (values not shown) does not seem to improve obtained results as it is practically a constant term for FSE and PD1 ligands.

Table 6 Binding free energy values (kcal/mol) obtained with the MMPBSA analysis of the minimized structures

Ligand	CDK6_FSE	CDK6_AP9	CDK6_PD1
FSE	**−49.11**	−56.35	−45.59
AP9	−38.82	**−45.01**	−49.20
BYP	−42.62	−39.93	−39.70
2PU	−51.07	−53.40	−46.90
PD1	−37.77	−47.66	**−43.32**

Bold values correspond to the X-ray complexes

Table 7 Binding free energy values (kcal/mol) obtained with the MMGBSA (igb = 2) analysis of the minimized structures

Ligand	CDK6_FSE	CDK6_AP9	CDK6_PD1
FSE	**−54.11**	−55.54	−47.25
AP9	−52.01	**−55.23**	−55.30
BYP	−52.62	−47.70	−52.00
2PU	−60.37	−65.58	−57.27
PD1	−50.78	−57.90	**−52.13**

Bold values correspond to the X-ray complexes

Despite force field calculations consider a completely flexible receptor, different starting structures lead to different minimized complexes with their corresponding ΔG values. Now, backbone movements are also allowed during the last steps of energy minimization. However, differences in ΔG values obtained for a given ligand docked to the different receptor structures used suggest that rearrangements produced after structural relaxation are not always enough to reproduce the X-ray experimental structure. This fact is clearly reflected for MMPBSA (see Table 6) and MMGBSA (see Table 7) values obtained for the cross-docking experiments. As it can be seen, considerable differences can be found in binding free energies calculated for the same ligand positioned into different receptor conformations. These differences are especially remarkable for the smallest ligand (FSE) docked on the receptors bonded to the other ligands and for the biggest ligands (AP9 and PD1) docked on the FSE receptor. Surprisingly, FSE is more stable in complex with the AP9 receptor than in complex with its own receptor. These differences are also observed with the GB approximation but in a softened manner. Also, it is important to note that the stability ranking for each receptor conformation (each column in Tables 6, 7) does not agree with the experimental order. In particular, in the case of the MMPBSA approach, the FSE ligand is predicted to exhibit a better binding energy than the PD1 ligand for the three considered receptor conformations.

Improper estimations of the binding free energy provided by the MMPBSA or the MMGBSA approximations could be attributed to the lack of conformational sampling. Hence, molecular dynamics were performed in order to extract a number of relevant conformations and calculate a mean value for ΔG. To increase this conformational sampling, two approaches were considered. The typical one consists of running a single molecular dynamics calculation of 5 ns for each complex from which ΔG values are extracted. ΔG values for each snapshot during the molecular dynamics run have been depicted (as shown in Figs. 4, 5), exhibiting stable values typical of a converged structure. However, it has recently been discussed [37] that different short molecular dynamics runs can lead to a more diverse conformational sampling. For that reason, a second approach was essayed that included five short molecular dynamics runs of 1 ns for each optimized structure. ΔG was calculated for each dynamics run, and mean values were used as a representative score of the system.

As shown in Table 8, the use of different conformations obtained from a molecular dynamics run of the X-ray complexes does not seem to improve the ranking of the theoretical binding free energy. However, changes observed from the use of multiple molecular dynamics seem to follow the right trend. Despite the affinity ranking

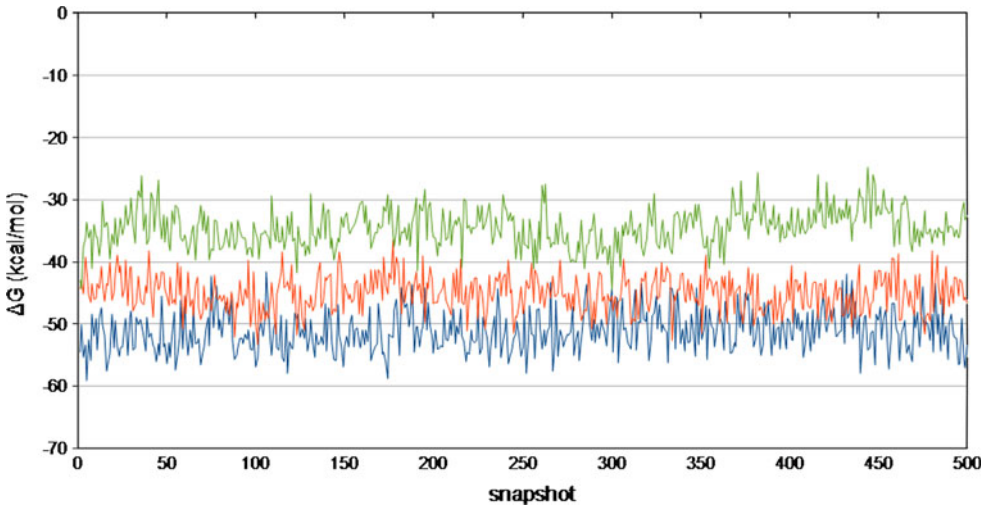

Fig. 4 Binding free energy values obtained from the MMPBSA approach for the 5-ns molecular dynamics for the FSE, PD1, and AP9 complexes in *blue*, *red*, and *green*, respectively

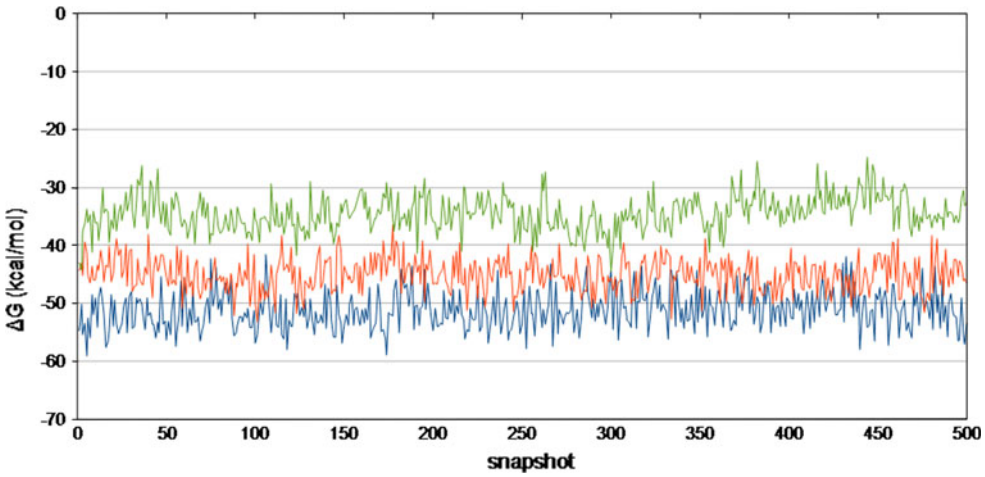

Fig. 5 Binding free energy values obtained from the MMGBSA (igb = 2) approach for the 5-ns molecular dynamics for the FSE, PD1, and AP9 complexes in *blue*, *red*, and *green*, respectively

Table 8 Binding free energy values (kcal/mol) obtained from the MMPBSA/MMGBSA calculation

Method	Approach	CDK6_FSE	CDK6_AP9	CDK6_PD1
MMPBSA	1 MD 5 ns	**−51.54**	**−20.60**	**−34.61**
	MD 1 1 ns	−43.92	−32.14	−33.49
	MD 2 1 ns	−48.95	−29.80	−33.21
	MD 3 1 ns	−51.88	−32.28	−36.37
	MD 4 1 ns	−45.80	−28.37	−35.87
	MD 5 1 ns	−47.11	−28.07	−34.92
	Mean MD 1 ns	**−47.53**	**−30.13**	**−34.77**
MMPGBSA	1 MD 5 ns	**−51.19**	**−34.50**	**−45.06**
	MD 1 1 ns	−46.34	−42.57	−43.58
	MD 2 1 ns	−50.34	−41.69	−43.22
	MD 3 1 ns	−52.04	−40.88	−46.76
	MD 4 1 ns	−48.01	−38.27	−46.63
	MD 5 1 ns	−48.92	−44.27	−46.17
	Mean MD 1 ns	**−49.13**	**−41.54**	**−45.27**

Different approaches were used for conformational sampling. Values in bold correspond to the mean ΔG of the 5-ns molecular dynamics runs and the mean of the 5 molecular dynamics of 1 ns

is maintained, the theoretical binding free energy of the FSE inhibitor becomes worse, whereas the AP9 binding energy improves, which is consistent with experimental IC_{50} values. The PD1 inhibitor practically preserves its estimated binding free energy. Thus, when comparing with the single molecular dynamics procedure, theoretical values obtained with this methodology are closer to the experimental results.

However, none of the two approaches considered for the conformational sampling leads to a proper ranking of the three ligands, as FSE still remains predicted as an excessively good inhibitor. Thus, it can be concluded that despite the conformational sampling influences the estimation of the binding free energy, there are also methodology factors that lead to improper results in the compound ranking.

3.3.1 MMPB/GBSA contributions

The different terms that compose the MMPB/GBSA equation for the minimized structures were analyzed in order to determine which ones could be responsible for the

miscorrelation between theoretical and experimental affinity values.

Firstly, only results for X-ray structures were analyzed. It can be seen (see bold values in Table 9) that gas-phase electrostatic interactions (ELE) are clearly favorable for the smallest ligand and that there is an opposite trend when comparing with experimental results. Oppositely, gas-phase van der Waals interactions (VDW) are favorable for the biggest ligand, and for this case, compounds are properly ranked. Polar solvation terms (PBCAL or GB) are similar for the three complexes and unfavorable to the binding process. Non-polar solvation terms (PBSUR or GBSUR) have small absolute values but exhibit trends in agreement with experimental data.

In addition, partial sum of electrostatic interactions (GBELE or PBELE, respectively), corresponding to electrostatic energy in gas phase (ELE) plus polar solvation terms (PBCAL or GBCAL) were calculated (see bold values in Table 10a, c). Highly unfavorable values were found for all ligands except FSE. This fact is in complete disagreement with experimental IC_{50} values, and inclusion of the van der Waals terms in the total binding free energy is not enough to properly rank complexes. When considering only the sum of hydrophobic interactions (PBVDW

Table 9 Different terms of the MMPB/GBSA approach (kcal/mol)

Ligand	CDK6_FSE	CDK6_AP9	CDK6_PD1
(a) ELE			
FSE	**−55.49**	−67.87	−54.60
AP9	−26.28	**−35.35**	−27.89
BYP	−25.94	−38.31	−31.91
2PU	−51.09	−54.63	−42.26
PD1	−18.98	−21.85	**−18.88**
(b) VDW			
FSE	**−36.73**	−33.43	−32.45
AP9	−58.59	**−53.44**	−57.96
BYP	−58.73	−54.38	−54.76
2PU	−53.29	−55.21	−55.70
PD1	−70.35	−70.49	**−67.15**
(c) PBCAL			
FSE	**47.28**	49.34	45.96
AP9	51.81	**49.56**	42.57
BYP	47.62	58.61	52.92
2PU	58.54	61.81	56.58
PD1	57.42	50.90	**48.72**
(d) PBSUR			
FSE	**−4.17**	−4.38	−4.50
AP9	−5.76	**−5.79**	−5.92
BYP	−5.57	−5.85	−5.95
2PU	−5.22	−5.37	−5.53
PD1	−5.87	−6.22	**−6.01**
(e) GB			
FSE	**41.13**	48.96	43.11
AP9	37.34	**38.08**	35.16
BYP	36.41	49.58	39.38
2PU	47.95	48.37	44.98
PD1	43.12	39.28	**38.63**
(f) GBSUR			
FSE	**−3.02**	−3.20	−3.30
AP9	−4.48	**−4.51**	−4.60
BYP	−4.36	−4.60	−4.71
2PU	−3.94	−4.12	−4.29
PD1	−4.57	−4.84	**−4.74**

Table 10 Total electrostatic and van der Waals contributions (kcal/mol)

Ligand	CDK6_FSE	CDK6_AP9	CDK6_PD1
(a) PBELE = ELE + PBCAL			
FSE	**−8.21**	−18.53	−8.64
AP9	25.53	**14.21**	14.68
BYP	21.68	20.30	21.01
2PU	7.45	7.18	14.32
PD1	38.44	29.05	**29.84**
(b) PBVDW = VDW + PBSUR			
FSE	**−40.90**	−37.81	−36.95
AP9	−64.35	**−59.23**	−63.88
BYP	−64.30	−60.23	−60.71
2PU	−58.51	−60.58	−61.23
PD1	−76.22	−76.71	**−73.16**
(c) GBELE = ELE + GB			
FSE	**−14.36**	−18.91	−11.49
AP9	11.06	**2.73**	7.27
BYP	10.47	11.27	7.47
2PU	−3.14	−6.26	2.72
PD1	24.14	17.43	**19.75**
(d) GBVDW = VDW + GBSUR			
FSE	**−39.75**	−36.63	−35.75
AP9	−63.07	**−57.95**	−62.56
BYP	−63.09	−58.98	−59.47
2PU	−57.23	−59.33	−59.99
PD1	−74.92	−75.33	**−71.89**

Gas and solvation terms are included (a) PBELE = ELE + PBCAL; (b) PBVDW = VDW + PBSUR; (c) GBELE = ELE + GB; and (d) GBVDW = VDW + GBSUR

and GBVDW), van der Waals interaction energy in gas-phase (VDW) and non-polar solvation terms (PBSUR or GBSUR), an improved ranking can be obtained (see bold values in Table 10b, d).

In the case of cross-receptor calculations, as different structures resulted from minimization of different starting complexes, binding free energy terms estimated for a given ligand in each receptor conformation are not completely equivalent. Indeed, dispersion in the ELE values has a maximum of 13 kcal/mol, which is very similar to what is observed for PBCAL or GB values. However, VDW values are within a narrow range (about 4 kcal/mol) as PBSUR or GBSUR contributions vary only within the range of 1 kcal/mol. Results point that VDW contributions are practically equivalent among all the complexes, whereas electrostatic contributions considerably differ. These conclusions can be also applied to the PBELE, GBELE, PBVDW, and GBVDW values.

When focusing on rankings obtained for each receptor conformation, it can be seen that no correlation between experimental data and electrostatic values, in any of their contributing terms, is observed. However, PBVDW and GBVDW values reasonably correlate with experimental activities. For the AP9 receptor, results are in complete agreement with IC_{50}, whereas results fail with the AP9 ligand in the case of the PD1 receptor and do not correlate at all in the case of the FSE receptor. This fact suggests that the narrow binding pocket of the FSE X-ray structure is not able to accommodate big ligands, such as AP9 or PD1, and may need extra optimization steps to complete the rearrangements needed. Also, as it can be seen in Fig. 2, the AP9 receptor pocket is bigger than the pockets of the two other receptors. This fact is related not only to the size of the ligands but also to the structure of the experimental X-ray pose for the ligands.

As van der Waals contributions were similar for the three complexes considered for each ligand, mean values were calculated seeking for better results. When using mean values (available in supporting information), VDW energies, as well as their sums with solvation non-polar terms (PBVDW and GBVDW), are not in agreement with experimental data. As the values extracted from calculations on the complexes of the FSE receptor are included in the mean calculation, unreasonable values for some ligands do not allow obtaining a proper ranking. However, mean values calculated only for the PD1 and AP9 receptor do not seem to improve the results because of the high value assigned to the AP9 ligand on the PD1 receptor.

As it has been discussed, improper performance of the MMPB/GBSA score is mainly due to the electrostatic contribution. In addition, including only the van der Waals contribution seems to allow correlation with experimental activities, at least for some receptors. These facts suggest that the parametrization used for the calculations may overestimate electrostatic contributions leading to improper results. Thus, as has been suggested recently [38], increasing the contribution of hydrophobic terms should balance both contributions and provide more realistic values.

For this purpose, the value of the γ parameter used in the calculation of the non-polar solvation term in the PB approximation was modified in order to increase the van der Waals contribution to the binding free energy, varying from a twofold to a 24-fold of the original value ($\gamma_0 = 0.00542$). Differences in the ΔG value due to an increase in the γ parameter are especially remarkable for AP9 and PD1 in comparison with changes produced in FSE, which exhibits a smaller solvent-accessible surface area.

Considering the minimized structures, the computed binding energy decreases linearly for higher γ values (Fig. 6 and values in Table 11). As discussed before, a softened trend is observed for the FSE inhibitor, which should be considered the most potent from the previous calculations. This fact allows us to conclude that for γ values higher than $6\gamma_0$, the ranking provided by MMPBSA is in agreement with the experimental data. However, from an experimental point of view, PD1 activity is considerably higher than AP9 one. Thus, only γ values higher than $16\gamma_0$ can discern these two compounds which have just a 2 kcal/mol difference in binding affinity.

When using the conformations extracted from the 5-ns molecular dynamics run, a better performance of the MMPB/GBSA function is obtained (Fig. 7 and values in Table 12). Starting values of the γ parameter already discern the higher affinity of the PD1 inhibitor in comparison with AP9. Hence, only the ranking position for the FSE inhibitor has to be modified. In this case, higher γ values are needed to rank compounds in agreement with experimental data. When using a γ value of $20\gamma_0$, an equivalent binding affinity is obtained for FSE and AP9, which is consistent with the experimental IC_{50} (850 and 450 nM, respectively). However, a γ value of $22\gamma_0$ leads also to a proper ranking, but now discerning these two compounds.

In the case of the 5 molecular dynamics runs of 1 ns, only the best γ values found were analyzed (values shown in Table 13). Mean values were calculated from the MMPB/GBSA values of the five molecular dynamics runs. Despite in this case AP9 binding affinity is closer to the PD1 value instead of the FSE one, the compound ranking agrees with the experimental affinities.

From all these calculations, it can be concluded that a higher γ value is needed in order to properly rank compounds. Binding energies calculated from either minimized or molecular dynamics conformations are now in good agreement with experimental data when the optimal

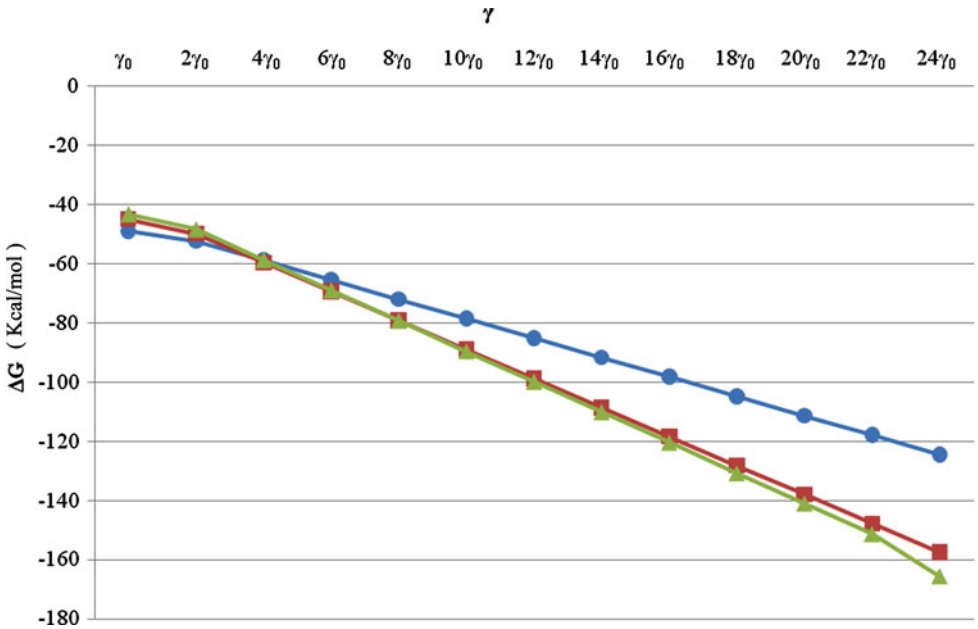

Fig. 6 MMPBSA values obtained for the minimized X-ray structures as a function of the γ parameter in the calculation of the non-polar solvation terms. FSE complex is shown with *filled circles*, AP9 with *filled squares*, and PD1 with *filled triangles*

Table 11 MMPBSA values for the three X-ray minimized structures (kcal/mol) calculated using different values for the γ parameter in the calculation of the non-polar solvation terms

γ	FSE	AP9	PD1
γ_0	−49.14	−45.04	−43.36
$2\gamma_0$	−52.41	−49.93	−48.50
$4\gamma_0$	−58.96	−59.72	−58.77
$6\gamma_0$	−65.51	−69.51	−69.05
$8\gamma_0$	−72.06	−79.30	−79.32
$10\gamma_0$	−78.61	−89.09	−89.60
$12\gamma_0$	−85.17	−98.87	−99.87
$14\gamma_0$	−91.72	−108.66	−110.14
$16\gamma_0$	−98.27	−118.45	−120.42
$18\gamma_0$	−104.82	−128.24	−130.69
$20\gamma_0$	−111.42	−138.03	−140.96
$22\gamma_0$	−117.92	−147.82	−151.24
$24\gamma_0$	−124.47	−157.61	−165.51

Values in bold correspond to the γ value that allows discerning FSE and AP9 considering a difference of 2 kcal/mol in their binding energy. $\gamma_0 = 0.00542$ is considered

determined γ values are used. However, conformational sampling derived from the longest molecular dynamics runs seems to lead to more realistic relative MMPB/GBSA values.

Cross-dockings for the five studied ligands into the three receptor conformations were analyzed for minimized structures. MMPB/GBSA binding free energies were determined for the 15 possible complexes using the optimal γ value found from previous calculations. As shown in Table 14, a reasonable ranking is obtained for the three receptors. As happened for the docking studies, biggest ligands cannot be easily located into some conformations of the binding site. As can be seen for the FSE-bound receptor, these ligands (i.e., AP9 and PD1) have an improper position in the ranking of compounds. The same happens for the PD1-bound receptor when trying to dock the AP9 ligand; despite using energy minimization, the narrow cavities are not able to accommodate these ligands. Moreover, the position of BYP ligand in the ranking is still questionable. As previously discussed, the experimental IC_{50} corresponds to CDK4 inhibition, and thus, small disagreements with this ligand may be due to this uncertainty in its inhibition constant.

It can be thought that molecular dynamics at room temperature will include a higher degree of flexibility and thus allow the molecular rearrangements needed. However, macromolecular structural rearrangements often need a long molecular dynamics run time which implies a computationally expensive methodology. As the main goal of this work is to obtain a reliable methodology to dock and score compounds with similar binding affinities, the use of long molecular dynamics is discouraged.

In conclusion, it is worth pointing out that molecular dynamics leads to a better ligand ranking and also seems necessary to achieve the desired conformational changes needed inside the binding pocket in order to accommodate different ligands. However, when using a receptor with a big cavity, the ranking obtained using only energy minimization is in good agreement with experimental results. Moreover, the computational cost required by this methodology can be afforded in order to rank potential inhibitors or modifications of known hits, typical problems stated by the drug discovery process.

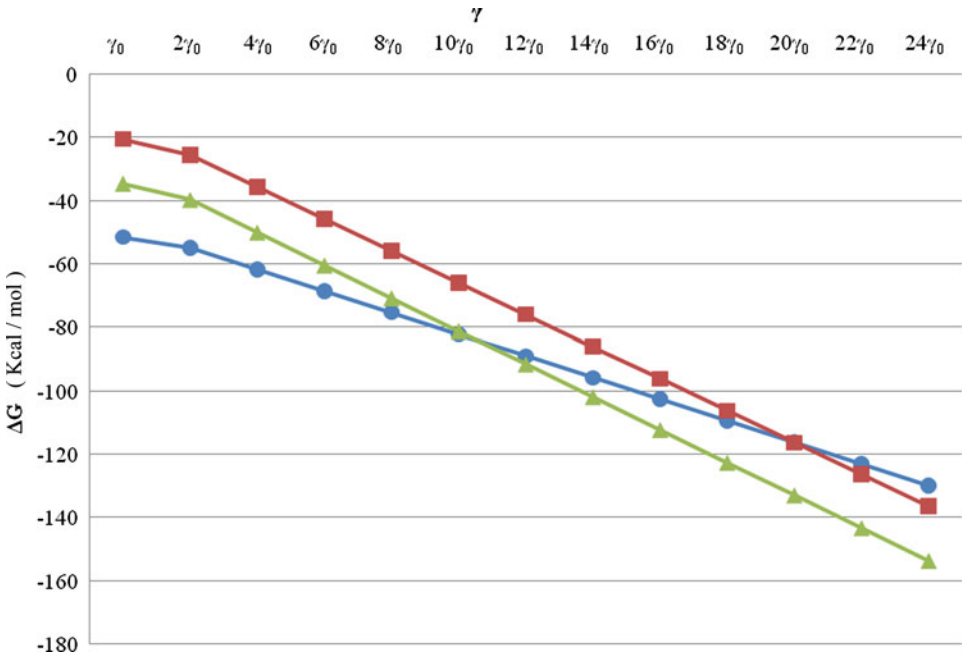

Fig. 7 MMPBSA values obtained for the 5-ns molecular dynamics of the X-ray structures as a function of the γ parameter in the calculation of the non-polar solvation terms. FSE complex is shown with *filled circles*, AP9 with *filled squares*, and PD1 with *filled triangles*

Table 12 Mean MMPBSA values (kcal/mol) for the conformations extracted from the 5-ns molecular dynamics run for the X-ray complexes

γ	FSE	AP9	PD1
γ_0	−51.55	−20.58	−34.61
$2\gamma_0$	−54.96	−25.63	−39.79
$4\gamma_0$	−61.78	−35.71	−50.15
$6\gamma_0$	−68.59	−45.80	−60.51
$8\gamma_0$	−75.41	−55.88	−70.87
$10\gamma_0$	−82.23	−65.97	−81.23
$12\gamma_0$	−89.04	−76.05	−91.59
$14\gamma_0$	−95.86	−86.14	−101.95
$16\gamma_0$	−102.67	−96.22	−112.31
$18\gamma_0$	−109.49	−106.31	−122.68
$20\gamma_0$	**−116.31**	**−116.40**	**−133.04**
$22\gamma_0$	**−123.12**	**−126.48**	**−143.40**
$24\gamma_0$	−129.94	−136.57	−153.76

Values are calculated using different values for the γ parameter in the calculation of the non-polar solvation terms. The first row in bold corresponds to the γ value that leads to an equivalent binding energy for FSE and AP9, according to their experimental affinities. The second corresponds to the γ parameter that allows to slightly discern the binding energies of FSE and AP9. $\gamma_0 = 0.00542$ is considered

Table 13 MMPBSA mean values (kcal/mol) of the conformations extracted from the five 1-ns molecular dynamics runs of the X-ray complexes

Ligand	FSE	AP9	PD1
(a)			
MD1	−111.54	−126.79	−133.70
MD2	−114.47	−127.14	−133.08
MD3	−117.13	−129.18	−137.81
MD4	−112.18	−118.69	−134.80
MD5	−113.36	−123.78	−135.08
Mean	**−113.74**	**−125.12**	**−134.89**
(b)			
MD1	−118.66	−136.75	−144.25
MD2	−121.36	−137.39	−143.60
MD3	−124.00	−139.38	−148.49
MD4	−119.16	−128.20	−145.21
MD5	−120.34	−133.86	−145.63
Mean	**−120.70**	**−135.12**	**−145.44**

Values in bold correspond to the mean binding energy calculated from five molecular dynamics runs. For the calculation of the non-polar solvation terms, γ parameters used were optimal values found from molecular dynamics calculations: (a) $\gamma = 20\gamma_0$ and (b) $\gamma = 22\gamma_0$. $\gamma_0 = 0.00542$ is considered

4 Conclusions

In the preclinical phase of drug discovery, hit discovery requires optimization of the affinity and ADME properties as well as lowering toxicity levels to identify lead compound candidates for clinical development. The main challenge from this "hit-to-lead" stage relies on the accuracy of docking methods to dock and score compounds, especially when the ligand set considered presents a narrow range of binding affinities. In fact, accuracy of docking methods depends not only on the scoring function used to rank the poses but also on the ability of the docking method

Table 14 MMPBSA values (kcal/mol) for the minimized structures of the five analyzed ligands docked into the three conformations of the CDK6 receptor using $16\gamma_0$ as value for the γ parameter

Ligand	CDK6_FSE	CDK6_AP9	CDK6_PD1
FSE	**−98.27**	−108.41	−99.21
AP9	−111.65	**−118.45**	−124.07
BYP	−113.63	−114.80	−116.37
2PU	−115.10	−120.38	−116.62
PD1	−112.04	−126.25	**−120.42**

$\gamma_0 = 0.00542$ is considered

to reproduce the experimental binding mode, being the correct depiction of receptor flexibility still one of the major challenges. At this purpose, the performance of different approximations to properly dock and score compounds with known activity in a narrow range of IC_{50} values was analyzed.

Different-sized receptor cavities were considered from the three X-ray available receptor conformations, and the inclusion of different degrees of flexibility in the binding site region was expected to be determinant in the docking results. None of the docking methodologies considered (neither the rigid receptor approach considered by Glide nor the sidechain rearrangements allowed by Induced Fit Docking) with any of their scoring functions were able to reproduce the experimental binding affinities for all ligands docked in the receptor conformations considered. Thus, it can be said that rearrangements allowed by the Induced Fit Docking are not enough to accommodate ligands into different-sized binding sites. Indeed, focusing only on re-docked experimental structures, it can be seen that results from Induced Fit Docking do not improve those obtained from the Glide rigid receptor approach.

Reasonable results were obtained when using the E-Model scoring function to select the docking pose. Theoretical rankings obtained for all receptor conformations were in good agreement with experimental data. Discrepancies found in this case corresponded always to docking runs where ligand and binding site have relatively different sizes. Hence, as it has been previously discussed, flexibility introduced by sidechain mobility is not enough to achieve the ligand-optimal interactions. Thus, it can be concluded that, despite binding affinities are usually related to interaction energies, in this case, the score obtained by the grid stage with ligand strain energy seems to be the best choice to reproduce binding affinities. However, more work is needed to confirm these results.

As regards docking results, it can be said that there are some considerations that must be taken into account in order to obtain reliable docking results. A proper compound ranking only makes sense when the structures to be scored mimic the experimental binding mode. Thus, in order to achieve docking results similar to experimental binding modes, a model energy score function must be used and isolated poses discarded. In addition, reasonable docking results are only obtained when the binding cavity and the battery of ligands docked have similar sizes. Hence, when there are several receptor conformations available, the one whose cavity is similar to the ligand size must be selected to perform the docking assays.

Docking results were also compared to results obtained from force field calculations. The lack of correlation between the ΔG calculated using the minimized X-ray structures and the experimental binding affinities denotes an improper performance of the MMPB/GBSA methodology. The extension of the free energy analysis to a set of complex conformations obtained from molecular dynamics simulations does not seem to be the reason for the miscorrelation observed. This fact suggests that there are other methodology factors that lead to an improper compound ranking. Specifically, no correlation was found between electrostatic terms of the MMPB/GBSA approach. Thus, despite van der Waals terms reasonably rank the compounds, this contribution is not enough to determine the final ordering.

In order to balance electrostatic and van der Waals contributions, the γ value of the non-polar solvation term was increased. Then, theoretical binding free energies from minimized and molecular dynamics conformations were analyzed for different γ values. From these calculations, it can be concluded that a higher γ value is needed to properly rank the compounds, either for minimized complexes or for molecular dynamics conformations. In addition, conformational sampling derived from molecular dynamics trajectories seems to provide more realistic results, especially for long molecular dynamics runs. This fact can be attributed to the time needed by macromolecules to achieve the structural rearrangements needed. Metadynamics or self-guided Langevin molecular dynamics methods should improve the performance of the MMPB/GBSA methodology. However, the computational cost of this kind of methodologies makes its use unaffordable for a standard lead discovery process.

In conclusion, it must be said that some conformational changes are needed for cross-docking results in order to achieve the optimal ligand interactions. This suggests that computationally expensive methods would be required to achieve structural rearrangements and thus to obtain a reliable binding energy value. However, for large receptor cavities, a proper ranking can be obtained with a simple complex relaxation.

Acknowledgments The Spanish Ministry of Science and Technology supported this work through project CTQ2006-06588/BQU. This

work was also supported in part by the *Generalitat de Catalunya* through project 2009SGR1308. We are also grateful to the *Departament d'Universitat, Recerca i Societat de la informació de la Generalitat de Catalunya i del Fons Social Europeu.*

References

1. Malumbres M, Barbacid M (2009) Cell cycle, CDKs and cancer: a changing paradigm. Nat Rev Cancer 9(3):153–166
2. Galons H, Oumata N, Meijer L (2010) Cyclin-dependent kinase inhibitors: a survey of recent patent literature. Expert Opin Ther Pat 20(3):377–404
3. Massague J (2004) G1 cell-cycle control and cancer. Nature 432(7015):298–306
4. Toogood PL et al (2005) Discovery of a Potent and Selective Inhibitor of Cyclin-Dependent Kinase 4/6. J Med Chem 48(7): 2388–2406
5. Lapenna S, Giordano A (2009) Cell cycle kinases as therapeutic targets for cancer. Nat Rev Drug Discov 8(7):547–566
6. Malumbres M et al (2008) CDK inhibitors in cancer therapy: what is next? Trends Pharmacol Sci 29(1):16–21
7. Leach AR, Shoichet BK, Peishoff CE (2006) Prediction of protein-ligand interactions. Docking and scoring: successes and gaps. J Med Chem 49(20):5851–5855
8. Cheng T et al (2009) Comparative assessment of scoring functions on a diverse test set. J Chem Inf Model 49(4):1079–1093
9. Duca JS, Madison VS, Voigt JH (2008) Cross-docking of inhibitors into CDK2 structures. 1. J Chem Inf Model 48(3): 659–668
10. Voigt JH et al (2008) Cross-docking of inhibitors into CDK2 structures 2. J Chem Inf Model 48(3):669–678
11. Schrödinger (2009) Glide, version 5.5. New York
12. Schrödinger (2010) Maestro, version 9.1. New York
13. Schrödinger (2009) Induced Fit Docking protocol (Schrödinger Suite 2009). New York, NY. p. Schrödinger Suite 2009: Glide version 5.5, Schrödinger, LLC, New York, NY, 2009; Prime version 2.1, Schrödinger, LLC, New York, NY, 2009
14. Kollman PA et al (2000) Calculating structures and free energies of complex molecules: combining molecular mechanics and continuum models. Acc Chem Res 33(12):889–897
15. Lu H et al (2005) Crystal structure of a human cyclin-dependent kinase 6 complex with a flavonol inhibitor, fisetin. J Med Chem 48(3):737–743
16. Lu H, Schulze-Gahmen U (2006) Toward understanding the structural basis of cyclin-dependent kinase 6 specific inhibition. J Med Chem 49(13):3826–3831
17. Beattie JF et al (2003) Cyclin-dependent kinase 4 inhibitors as a treatment for cancer. Part 1: Identification and optimisation of substituted 4, 6-bis anilino pyrimidines. Bioorg Med Chem Lett 13(18):2955–2960
18. Ikuta M et al (2001) Crystallographic approach to identification of cyclin-dependent kinase 4 (CDK4)-specific inhibitors by using CDK4 Mimic CDK2 protein. J Biol Chem 276(29):27548–27554
19. Schulze-Gahmen U, Jung JU, Kim SH (1999) Crystal structure of a viral cyclin, a positive regulator of cyclin-dependent kinase 6. Structure 7(3):245–254
20. Jeffrey PD, Tong L, Pavletich NP (2000) Structural basis of inhibition of CDK-cyclin complexes by INK4 inhibitors. Genes Dev 14(24):3115–3125
21. Case DA et al (2005) The Amber biomolecular simulation programs. J Comput Chem 26(16):1668–1688
22. Viktor H et al (2006) Comparison of multiple Amber force fields and development of improved protein backbone parameters. Proteins Struct Funct Bioinform 65(3):712–725
23. Junmei W et al (2004) Development and testing of a general amber force field. J Comput Chem 25(9):1157–1174
24. William LJ et al (1983) Comparison of simple potential functions for simulating liquid water. J Chem Phys 79(2):926–935
25. Darden T, York D, Pedersen L (1993) Particle mesh Ewald: an N · log(N) method for Ewald sums in large systems. J Chem Phys 98(12):10089–10092
26. Schrödinger (2009) LigPrep, version 2.3. New York
27. Friesner RA et al (2006) Extra precision glide: docking and scoring incorporating a model of hydrophobic enclosure for protein-ligand complexes. J Med Chem 49(21):6177–6196
28. Sherman W et al (2006) Novel procedure for modeling ligand/receptor induced fit effects. J Med Chem 49(2):534–553
29. Schrödinger (2009) Glide 5.5 User Manual. Schrödinger Press
30. Hussain A, Melville JL, Hirst JD (2010) Molecular docking and QSAR of aplyronine A and analogues: potent inhibitors of actin. J Comput Aided Mol Des 24(1):1–15
31. Rodriguez A et al (2005) Assessment of the performance of cluster analysis grouping using pharmacophores as molecular descriptors. J Mol Struct Theochem 727(1–3):81–87
32. Berendsen HJC et al (1984) Molecular dynamics with coupling to an external bath. J Chem Phys 81(8):3684–3690
33. Ryckaert J-P, Ciccotti G, Berendsen HJC (1977) Numerical integration of the cartesian equations of motion of a system with constraints: molecular dynamics of n-alkanes. J Comput Phys 23(3):327–341
34. Onufriev A, Bashford D, Case DA (2000) Modification of the generalized born model suitable for macromolecules. J Phys Chem B 104(15):3712–3720
35. Jörg W, Peter SS, Still WC (1999) Optimization of Gaussian surface calculations and extension to solvent-accessible surface areas. J Comput Chem 20(7):688–703
36. Onufriev A, Bashford D, Case DA (2004) Exploring protein native states and large-scale conformational changes with a modified generalized born model. Proteins Struct Funct Bioinform 55(2):383–394
37. Sadiq SK et al (2010) Accurate ensemble molecular dynamics binding free energy ranking of multidrug-resistant HIV-1 proteases. J Chem Inf Model 50(5):890–905
38. Zhang X, Li X, Wang R (2009) Interpretation of the binding affinities of PTP1B inhibitors with the MM-GB/SA method and the X-score scoring function. J Chem Inf Model 49(4):1033–1048